Title

Self-assembly of a group I intron active site from its component tertiary structural domains.

Journal

RNA, 1(1)

ISSN

1355-8382

Authors

Doudna, JA

Cech, TR

Publication Date

1995-03-01

RNA (1995), *1*:36–45. Cambridge University Press. Printed in the USA.

Self-assembly of a Group I intron active site from its component tertiary structural domains

JENNIFER A. DOUDNA[1] and THOMAS R. CECH

Department of Chemistry and Biochemistry, Howard Hughes Medical Institute, University of Colorado, Boulder, Colorado 80309-0215, USA

ABSTRACT

The catalytic core of Group I self-splicing introns has been proposed to consist of two structural domains, P4–P6 and P3–P9. Each contains helical segments and conserved unpaired nucleotides, and the isolated P4–P6 domain has been shown to have substantial native tertiary structure. The proposed tertiary structure domains of the *Tetrahymena* intron were synthesized separately and shown to self-assemble into a catalytically active complex. Surprisingly, the concentration dependence of these reactions revealed that the domains interact with nanomolar apparent dissociation constants, even though there is no known base pairing between P4–P6 and P3–P9. This suggests that the domains interact through multiple tertiary contacts, the nature of which can now be explored in this system. For example, a circularly permuted version of the P4–P6 domain, which folds similarly to the native P4–P6 molecule, formed a stable but inactive complex. Interestingly, activity was demonstrated with the permuted molecule when nucleotides proposed to form a triple-strand interaction with P4 and P6 were restored as part of the P1–P3 substrate or as part of the P3–P9 RNA. Thus, beyond stabilization of the P4–P6 domain, the triple-strand region may facilitate correct orientation of the RNA domains or participate more directly in catalysis.

Keywords: catalytic intron; ribozyme; RNA structure

INTRODUCTION

Several lines of evidence indicate that Group I self-splicing introns have a defined tertiary conformation required for catalysis. These introns bind two substrates during the course of catalysis, a guanosine nucleotide (or nucleoside) and an RNA duplex containing the exon–intron junctions (Cech, 1990). Highly specific contacts are made to each substrate by conserved nucleotides within the intron catalytic core (Michel et al., 1989a; Yarus et al., 1991; Pyle et al., 1992; Strobel & Cech, 1994). For example, tight binding of the 5′ exon is facilitated by tertiary interactions to specific 2′ hydroxyl groups on the backbone of the P1 helix. The Group I introns have a defined surface and an internal region that becomes protected from cleavage reagents upon addition of magnesium ions (Latham & Cech, 1989; Celander & Cech, 1991; Heuer et al., 1991). Crosslinking, chemical modification and cleavage studies, and mutational analysis have revealed several long-range structural interactions that are necessary for ribozyme function (Michel et al., 1990; Downs & Cech, 1990, 1994; Wang & Cech, 1992; Jaeger et al., 1993; Wang et al., 1993).

In parallel with the biochemical experiments, comparative sequence analysis has been used to derive a model for the catalytic core of Group I introns (Michel & Westhof, 1990; Michel et al., 1992). In this model, the core consists of two structural domains: P4–P6 is comprised of helical segments P4, P5, and P6, and P3–P9 is comprised of P3, P7, P8, and P9. The P4–P6 region contains approximately half of the conserved catalytic core, including nucleotides proposed to interact with the substrate helix (P1) during splicing (Wang et al., 1993). The other domain of the core, P3–P9, contains the guanosine binding site of the intron (Michel et al., 1989a). The binding site for the P1 substrate helix is thought to lie between the two domains, based on molecular modeling (Michel & Westhof, 1990) and photocrosslinking, affinity cleavage, and mutational analysis (Pyle et al., 1992; Wang & Cech, 1992; Wang et al.,

Reprint requests to: Thomas R. Cech, Department of Chemistry and Biochemistry, Howard Hughes Medical Institute, University of Colorado, Boulder, Colorado 80309-0215, USA; e-mail: cech@colorado.edu.

[1] Present address: Department of Molecular Biophysics and Biochemistry, Yale University, New Haven, Connecticut 06522, USA.

1993). A recent structural diagram that portrays these domains is shown in Figure 1 (Cech et al., 1994).

This model for the organization of these ribozymes is analogous to the structures of some proteins in which multiple structured regions, or domains, interact to create a catalytic center (i.e., Jacobson et al., 1994). In support of this idea, the P4–P6 region of the *Tetrahymena* intron was synthesized and shown by chemical mapping to fold into a stable tertiary structure on its own (Murphy & Cech, 1993). The chemical cleavage pattern was very similar to the pattern observed in this RNA within the context of the intron, leading to the proposal that P4–P6 is an independently folding domain. Further work identified certain regions of the P4–P6 RNA in which mutations disrupt the stability and conformation of the molecule, as assessed by chemical protection patterns (Murphy & Cech, 1994). Direct visualization of native and mutant P4–P6 RNA molecules was performed by electron microscopy, revealing a globular structure of the native RNA (Wang et al., 1994). The 160-nucleotide P4–P6 RNA is currently the subject of high-resolution X-ray crystallographic analysis (Doudna et al., 1993).

Although the structure of the P4–P6 domain has been studied extensively, there has been no means of testing its functional competence. Certain protein enzymes, such as β-galactosidase, are composed of multiple structural domains that can be separated and reconstituted in *trans*. RNA catalysts have in some cases also been divided into pieces that can associate by tertiary interactions to reassemble a functional unit (Jarrell et al., 1988; van der Horst et al., 1991; Dib-Hajj et al., 1993). Thus, the proposed domains of the *Tetrahymena* self-splicing intron were synthesized individually and assayed for function in a reconstitution reaction. We show here that these RNAs self-assemble into catalytically active complexes, and that they interact with nanomolar apparent dissociation constants. This system provides a useful method for assaying intron folding independently from intron activity, and we demonstrate how this will facilitate identification of tertiary contacts that contribute to catalysis.

RESULTS

To test whether the P4–P6 RNA could interact in *trans* with the P3–P9 region of the intron to reform the catalytic center, a new plasmid was constructed encoding the P3–P9 region separately (Fig. 1). Another template encoding P1–P3, which contains the 5′ splice site and 20 nucleotides of 5′ exon sequence, was prepared using

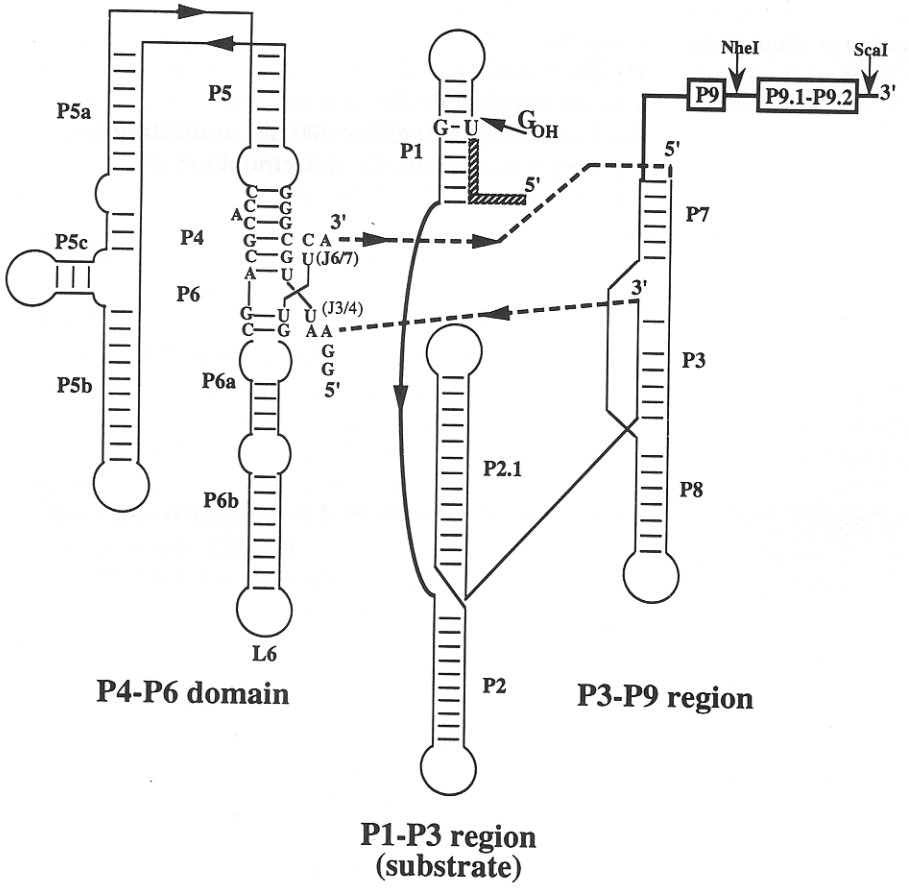

FIGURE 1. Schematic secondary structure of the Group I self-splicing intron from *Tetrahymena thermophila*. The proposed domains of the catalytic core are labeled P4–P6 and P3–P9, shown flanking the P1–P3 region, which contains the 5′ splice site and a 20-nucleotide exon sequence (hatched line). Two dashed lines show connectivities between domains in the intact intron that have been severed to produce the separate domains. Solid lines show connectivity within a separated domain molecule. Arrowheads superimposed on lines give 5′-to-3′ polarity. The 5′ cleavage site is indicated by an arrow showing guanosine attack. *Sca* I or *Nhe* I restriction enzyme cleavage of the template truncates the RNA as shown.

PCR. Because the P3 stem is formed by base-pairing between two distant parts of the sequence, it was necessary to separate it such that the 5′ strand of P3 is part of the P1–P3 RNA, whereas the 3′ strand is part of the P3–P9 RNA. Two versions of the P3–P9 RNA were prepared, P3–P9(*Sca* I), ending two nucleotides prior to the 3′ end of the intron, and P3–P9(*Nhe* I), ending within the P9.1 stem (see Fig. 1).

As an initial test of the ability of these three RNAs to assemble into an active complex, assays were performed with ~1 nM of radioactively labeled P1–P3 RNA in the presence of 100 nM each of the P4–P6 and P3–P9 RNAs and 5 mM guanosine triphosphate. Because P1–P3 contains the 5′ exon–intron junction in the P1 stem, a functional intron active site should catalyze guanosine attack at the labile phosphodiester bond, resulting in strand scission (Fig. 1). As shown in Figure 2, efficient cleavage of the P1–P3 substrate was observed at the expected position in the P1 stem when incubated with P4–P6 and P3–P9(*Sca* I). No reaction was observed in the presence of P4–P6 and the P3–P9(*Nhe* I) RNA (data not shown). Reaction did not occur in the absence of P4–P6 or P3–P9, or in the absence of guanosine. Although not requiring elevated magnesium and polyamine concentrations, reactivity was optimal with inclusion of 80 mM magnesium chloride and 5 mM spermidine in the reaction.

We next tested the strength of association of the RNA domains in the reaction. Because the P3 stem is a conserved element of the catalytic core, it was important to work under conditions where this stem was fully formed in a complex between P1–P3 and P3–P9. To identify appropriate concentrations of each RNA to produce a complex, radioactively labeled P1–P3 RNA (~1 nM) was incubated with increasing concentrations of unlabeled P3–P9 RNA for 10 min at 50 °C in reaction buffer. Electrophoresis in native polyacrylamide gels containing 10 mM $MgCl_2$ was used to separate unbound P1–P3 from P1–P3/P3–P9 complex (J.A. Doudna & T.R. Cech, unpubl. data). This analysis showed that complex formation was half complete between 25 and 50 nM of P3–P9 RNA (data not shown). Interestingly, the P3–P9(*Nhe* I) RNA was not observed to form a complex with P1–P3 even at micromolar concentrations. Likewise, no complex was observed between micromolar P3–P9(*Sca* I) RNA and a ^{32}P-labeled oligonucleotide of sequence 5′-GACCGUCA-3′ that could potentially base pair with the P3 sequence on P3–P9. These observations suggested that base pairing alone was insufficient for driving the formation of P3 at these RNA concentrations, so tertiary interactions presumably contributed to the association of P1–P3 and P3–P9. Our native gel analysis provided the basis for a set of kinetic experiments to measure the apparent dissociation constants of the component RNAs in the active complex.

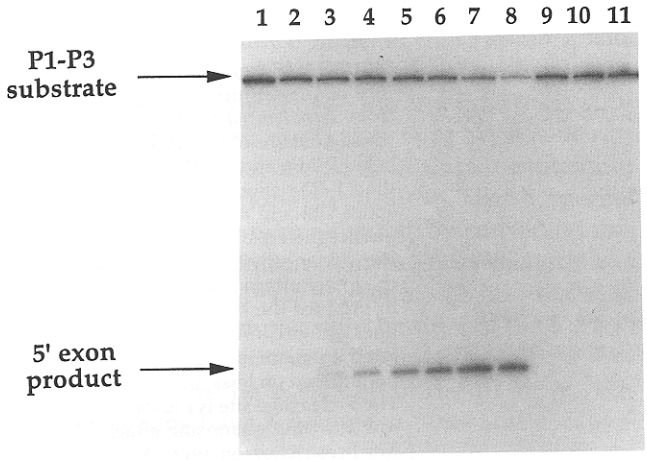

FIGURE 2. Time course for cleavage of the P1–P3 substrate RNA in a complex with the P4–P6 and P3–P9 RNAs. Approximately 1 nM of 5′-^{32}P-labeled P1–P3 RNA was incubated with 100 nM each of P4–P6 RNA and P3–P9(*Sca* I) RNA and 5 mM GTP in reaction buffer at 40 °C (see Materials and methods). Reaction products were analyzed on a 10% polyacrylamide gel containing 7 M urea, an autoradiogram of which is shown. Lanes 1–8, reaction products after incubation for 0, 1, 2, 5, 10, 20, 60, 120 min; lane 9, no P4–P6 RNA in reaction; lane 10, no P3–P9(*Sca* I) RNA in reaction; lane 11, no GTP in reaction. Lanes 9–11, reactions incubated for 120 min.

To measure the concentration dependence for P4–P6 RNA binding to the P1–P3/P3–P9 complex, time courses for P1–P3 cleavage were performed with 1 nM P1–P3, 100 nM P3–P9(*Sca* I) RNA and 0, 20, 70, 200, or 500 nM P4–P6 RNA. Initial rates of reaction at each P4–P6 concentration were determined and plotted versus P4–P6 concentration (Fig. 3A). From this analysis, the K_m for P4–P6 was estimated to be 30 nM. The same K_m value was obtained when the concentration of P3–P9 RNA in the reaction was 50 nM or 500 nM, indicating that our data represent a true K_m determination rather than a titration, where P3–P9 would be stoichiometrically bound by P4–P6. The K_m for P3–P9 within the active complex was measured in a similar way using 1 nM P1–P3 RNA, 100 nM P4–P6 RNA, and 0, 1, 2, 4, 10, 30, 70, and 200 nM P3–P9 RNA. The K_m for P3–P9 binding was estimated to be ~4 nM, as shown in Figure 3B. This was a surprisingly low K_m, given that the native gel analysis had indicated a requirement for a higher concentration of P3–P9 to saturate binding of P1–P3 (K_d = 25–50 nM). Perhaps the presence of P4–P6 provides tertiary contacts that enhance the association of P1–P3 with P3–P9, or $K_m \neq K_d$ for this interaction.

We next wanted to use this approach to test the functional competence of a circularly permuted version of the P4–P6 domain RNA in which the 5′ end of P4 is directly joined to the 3′ end of P6 by a phosphodiester bond; the 5′ and 3′ termini of the molecule are in the former loop L6 (Fig. 4A). This "P4–P6 fusion" molecule was originally constructed to test the idea that the P4 and P6 helical elements are coaxially stacked in the native domain structure. Fe(II)-EDTA cleavage, native gel electrophoresis, and electron microscopic visualization

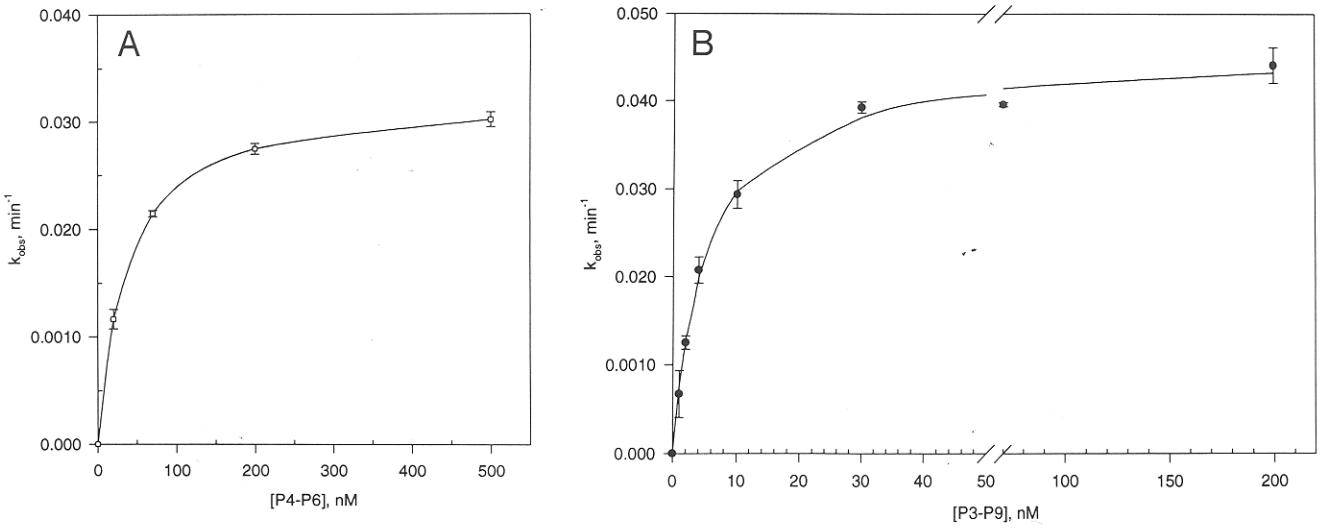

FIGURE 3. A: Initial rates of P1–P3 cleavage plotted as a function of P4–P6 RNA concentration in the reaction. Points on the curve represent rates measured with saturating (100 nM) P3–P9(*Sca* I) RNA in the reactions. Nearly identical curves were obtained for rates measured with either 50 nM or 500 nM P3–P9(*Sca* I) RNA in the reactions (data not shown). Error bars show standard deviation for data obtained from three independent experiments. The line represents a nonlinear least-squares fit to the data and gives a $K_m = 31 \pm 3$ nM. **B:** Initial rates of P1–P3 cleavage plotted as a function of P3–P9(*Sca* I) RNA concentration in the reaction. Rates were measured with saturating (100 nM) [P4–P6] in the reactions. Error bars show standard deviation for data obtained from three independent experiments. The line represents a nonlinear least-squares fit to the data and gives a $K_m = 4 \pm 0.5$ nM.

showed that, within the resolution limits of these techniques, the structure of the P4–P6 fusion molecule was indistinguishable from that of native P4–P6 domain RNA (Murphy et al., 1994). The P4–P6 fusion RNA was prepared and incubated with the other components of the intron complex as described above. However, no cleavage of the P1–P3 substrate could be detected, even at concentrations of the P4–P6 fusion RNA of 20 micromolar and long incubation times (>4 h) (data not shown).

The lack of reactivity could reflect an inability of the P4–P6 fusion molecule to bind to the complex, or it could result from inactivity of the complex. Binding of the P4–P6 fusion RNA was tested by measuring its inhibition of the reaction of 1 nM labeled P1–P3 RNA in the presence of 50 nM P3–P9 RNA and 30 nM P4–P6 RNA. Reactions were initiated with the addition of GTP as before, incubated for 15 min, and analyzed on a denaturing polyacrylamide gel (Fig. 4B). The P4–P6 fusion RNA specifically inhibited cleavage of the P1–P3 substrate RNA. No inhibition of the cleavage reaction was observed in the presence of 5 μM transfer RNA (tRNA), and only slight inhibition occurred with 125 μM tRNA in the reaction. The amount of inhibition at a range of concentrations of P4–P6 fusion RNA was plotted to determine a K_i of ~0.5 μM (Fig. 4C). Thus, binding is approximately 16-fold weaker than that observed for the native P4–P6 RNA, assuming that $K_m = K_d$ for the native P4–P6 RNA. Nevertheless, the affinity of the P4–P6 fusion molecule is within the range of the concentrations used to test for activity.

Because the P4–P6 fusion RNA is capable of binding to the domain complex but cannot react, we reasoned that the missing nucleotides in J3/4 and J6/7 might be required for function. These nucleotides are somewhat conserved in Group I introns and have been proposed to interact with the P4 and P6 stems, forming triple-stranded regions (Michel et al., 1990; Michel & Westhof, 1990; Chastain & Tinoco, 1992, 1993; Green & Szostak, 1994) (Fig. 5). Thus, it seemed possible that restoring this interaction might restore function with the P4–P6 fusion molecule. To test this idea, variants of the P1–P3 and P3–P9 RNAs were prepared, which included the J3/4 nucleotides on the 3′ end of P1–P3 (J3/4A) and the J6/7 nucleotides on the 5′ end of P3–P9. Two versions of the new P3–P9 RNA were designed, one beginning with two additional non-natural Gs at the 5′ end (J6/7GG) and the other with the J6/7 nucleotides changed from 5′-UCA to 5′-GCA (J6/7GC). These changes were necessary to facilitate transcription by T7 RNA polymerase, which requires at least one G at the 5′ end of the transcript. A new P4–P6 fusion RNA (fusion2) was designed with base pair 2 in P4 changed to allow a triple-helical interaction with J6/7GC according to the rules described by Michel et al. (1990) (Fig. 5).

Reactions with the new RNAs were performed as before, with 1 nM labeled P1–P3 or J3/4A RNA, 50 nM of the P3–P9 RNA, and either 50 nM P4–P6 RNA or 1 μM of P4–P6 fusion RNA. These concentrations of P4–P6 RNAs were used to compensate for the weaker binding of the P4–P6 fusion molecule. Cleavage products were separated on denaturing polyacrylamide gels,

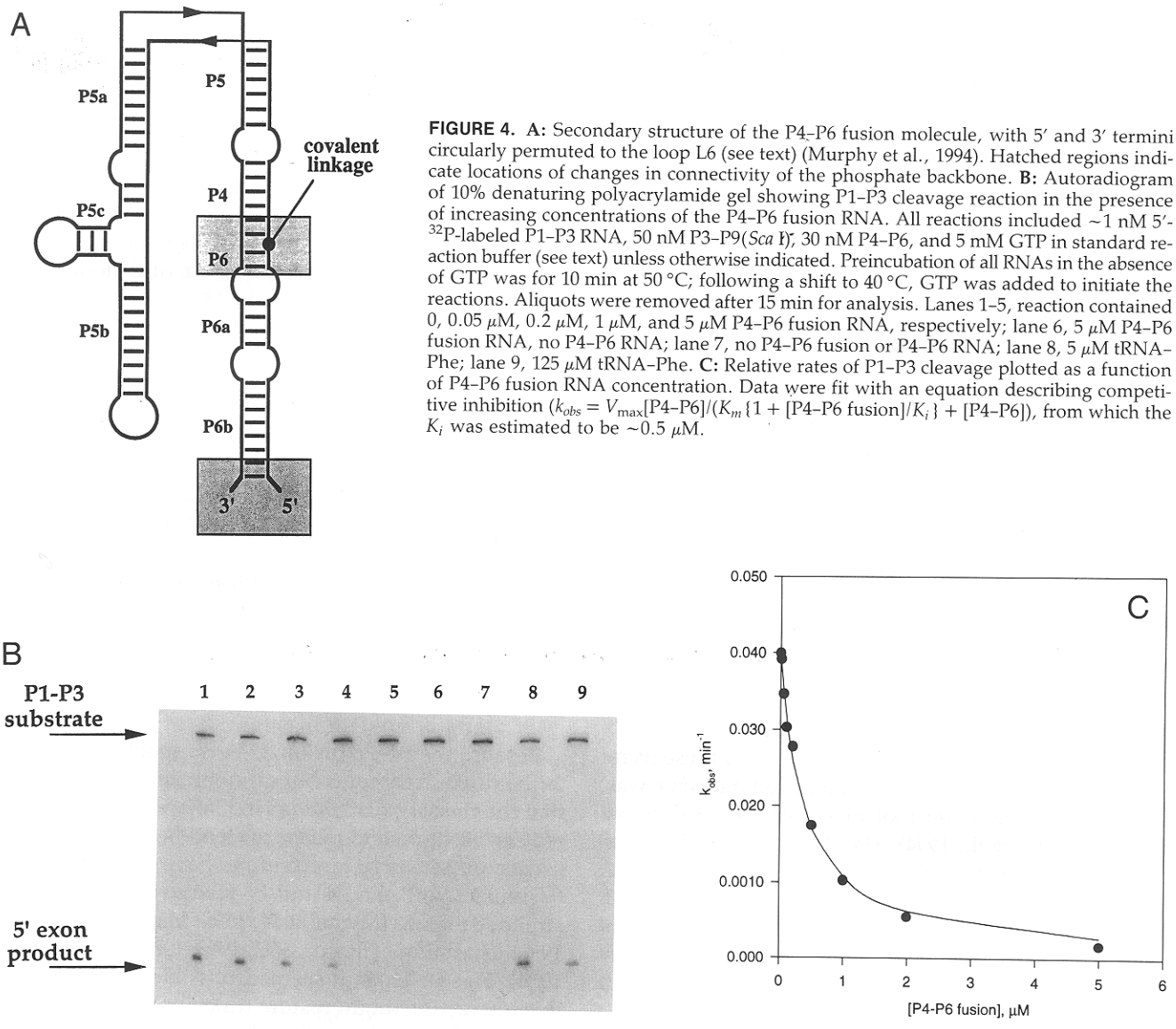

FIGURE 4. A: Secondary structure of the P4–P6 fusion molecule, with 5′ and 3′ termini circularly permuted to the loop L6 (see text) (Murphy et al., 1994). Hatched regions indicate locations of changes in connectivity of the phosphate backbone. **B:** Autoradiogram of 10% denaturing polyacrylamide gel showing P1–P3 cleavage reaction in the presence of increasing concentrations of the P4–P6 fusion RNA. All reactions included ~1 nM 5′-^{32}P-labeled P1–P3 RNA, 50 nM P3–P9(*Sca* I), 30 nM P4–P6, and 5 mM GTP in standard reaction buffer (see text) unless otherwise indicated. Preincubation of all RNAs in the absence of GTP was for 10 min at 50 °C; following a shift to 40 °C, GTP was added to initiate the reactions. Aliquots were removed after 15 min for analysis. Lanes 1–5, reaction contained 0, 0.05 μM, 0.2 μM, 1 μM, and 5 μM P4–P6 fusion RNA, respectively; lane 6, 5 μM P4–P6 fusion RNA, no P4–P6 RNA; lane 7, no P4–P6 fusion or P4–P6 RNA; lane 8, 5 μM tRNA-Phe; lane 9, 125 μM tRNA-Phe. **C:** Relative rates of P1–P3 cleavage plotted as a function of P4–P6 fusion RNA concentration. Data were fit with an equation describing competitive inhibition ($k_{obs} = V_{max}[\text{P4–P6}]/(K_m\{1 + [\text{P4–P6 fusion}]/K_i\} + [\text{P4–P6}])$, from which the K_i was estimated to be ~0.5 μM.

shown in Figure 6. With P4–P6 fusion RNA, no reaction was observed unless the J3/4 nucleotides were added back (J3/4A substrate; compare reactions b and d). The J6/7 nucleotides had a similar effect, but only in the case where J6/7 was changed such that no additional Gs were added to the 5′ end of P3–P9 (data not shown). When both J3/4 and J6/7 were present, cleavage occurred as well (reactions j and k, Fig. 6). Unnatural Gs on the 5′ end of the P3–P9 molecule (i.e., J6/7GG) inhibited the reaction (compare reactions d and e in Fig. 6). The sequences of the 5′ ends of J6/7GG and J6/7GC RNAs were confirmed by primer extension dideoxy sequencing to ensure that the differential effect on the reaction was not due to incorrect nucleotides in the J6/7 region (data not shown). Specific hydrolysis of the P1–P3 substrate RNA downstream from the normal 5′ splice site occurred during preincubation with some of the RNAs but did not affect interpretation of the results. Thus, the P4–P6 fusion domain does participate in a functional complex in the presence of J3/4 and/or J6/7, even though these joining regions are not covalently attached to P4 and P6.

DISCUSSION

The catalytic core of Group I self-splicing introns has been proposed to consist of two structural domains. One of these, P4–P6, was previously shown to fold into a stable tertiary structure both within the intron and when synthesized as a separate molecule (Murphy & Cech, 1993; Laggerbauer et al., 1994). We now find that the catalytic core can be reconstituted in *trans* by self-assembly of the two component domains along with a substrate RNA. The maximal rate of cleavage of the 5′ exon–intron junction in this complex is approximately 0.04 min^{-1}, which is 25-fold slower than that observed

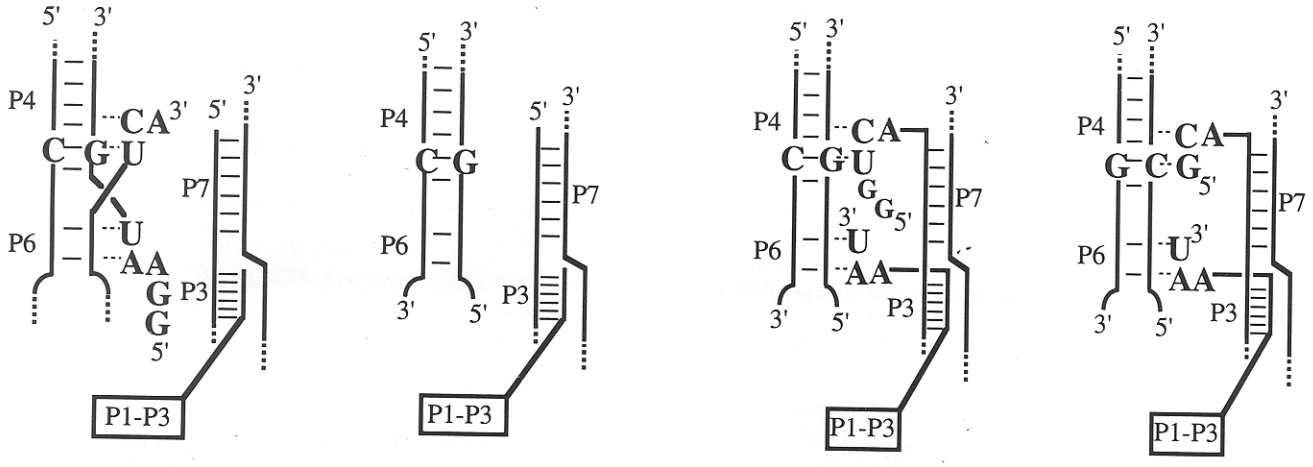

ACTIVE COMPLEX	INACTIVE COMPLEX	RECOVERY OF ACTIVITY	
wt P1-P3	wt P1-P3	J3/4A	J3/4A
wt P4-P6	P4-P6 fusion	P4-P6 fusion	P4-P6 fusion2
wt P3-P9	wt P3-P9	J6/7GG	J6/7GC

FIGURE 5. Proposed triple-stranded region in P4 and P6 of the Group I intron catalytic core. The original complex is diagrammed on the left; an inactive complex was formed with P4–P6 fusion RNA lacking the J3/4 and J6/7 nucleotides (see text). Recovery of activity of this complex was achieved by supplying the missing nucleotides as part of the other RNA components P1–P3 and P3–P9, as shown.

for the intact intron. This is remarkably good considering that three large RNAs must fold properly and bind in the correct orientations in the complex.

The reassembly of functional RNA macromolecules via base-pairing of complementary fragments is well known (Chambers, 1971; Uhlenbeck, 1987; Goldschmidt-Clermont et al., 1991). Group I introns have also been shown to assemble through base-pairing of complementary fragments (Szostak, 1986; Doudna et al., 1991). In the present work, however, there are no known base-pairing interactions between domains P4–P6 and P3–P9, and P4–P6 has so few single-stranded nucleotides that extensive base-pairing with P3–P9 is precluded. Comparative sequence analysis has not even revealed many candidates for the tertiary contacts that must exist to hold these RNA domains together (Michel & Westhof, 1990). Reassembly of active ribozymes from separate molecules through presumed tertiary interactions has been shown previously for a Group II intron (Jarrell et al., 1988; Dib-Hajj et al., 1993; Pyle & Green, 1994). Furthermore, the P5abc subdomain of the *Tetrahymena* intron can activate a truncated intron from which the subdomain had been deleted (van der Horst et al., 1991).

The strength of association of the *Tetrahymena* intron domains as judged from their K_m values (K_m = 30 nM for P4–P6, K_m = 4 nM for P3–P9; 80 mM $MgCl_2$, 5 mM spermidine, 40 °C) can be compared to other examples of RNA–RNA association that are thought to be mediated by tertiary interactions rather than base pairing. The RNA subunit of *Bacillus subtilis* RNase P binds its pre-tRNA^{Asp} substrate with K_d = 100 nM and binds the tRNA product with K_d = 3 nM (100 mM $MgCl_2$, 800 mM NH_4Cl, 37 °C; Beebe & Fierke, 1994). The isolated domain 5 of a Group II intron binds to an RNA comprised of the 5′ exon and domains 1–3 with K_d = 300–800 nM (100 mM $MgCl_2$, 500 mM KCl, 45 °C; Pyle & Green, 1994). A *Tetrahymena* ribozyme with P1 deleted binds an exogenous P1 substrate helix very weakly, $K_m > 0.1$ mM (20 mM $MgCl_2$, 10 mM NH_4Cl, 58 °C; Doudna & Szostak, 1989). Thus, assuming $K_m \approx K_d$, the association of the tertiary structural domains of the three-component ribozyme described here appears to be strong compared to previous examples of RNA tertiary structural interactions.

Like proteins, large structured RNA molecules may commonly be composed of smaller domains that can fold independently. For example, biochemical experiments and phylogenetic comparison indicate that both the Group II intron and ribonuclease P ribozymes contain multiple substructures that interact to form the active site (Michel et al., 1989b; Bachl & Schmelzer, 1990; Harris et al., 1994; Pan, 1994). In the case of ribosomal RNA, pieces of the RNA corresponding to secondary structure domains can bind ribosomal proteins (Kean & Draper, 1985; Weitzmann et al., 1993), and a degree of higher order structure or ligand-binding activity is maintained in some of these naked RNAs (Noller,

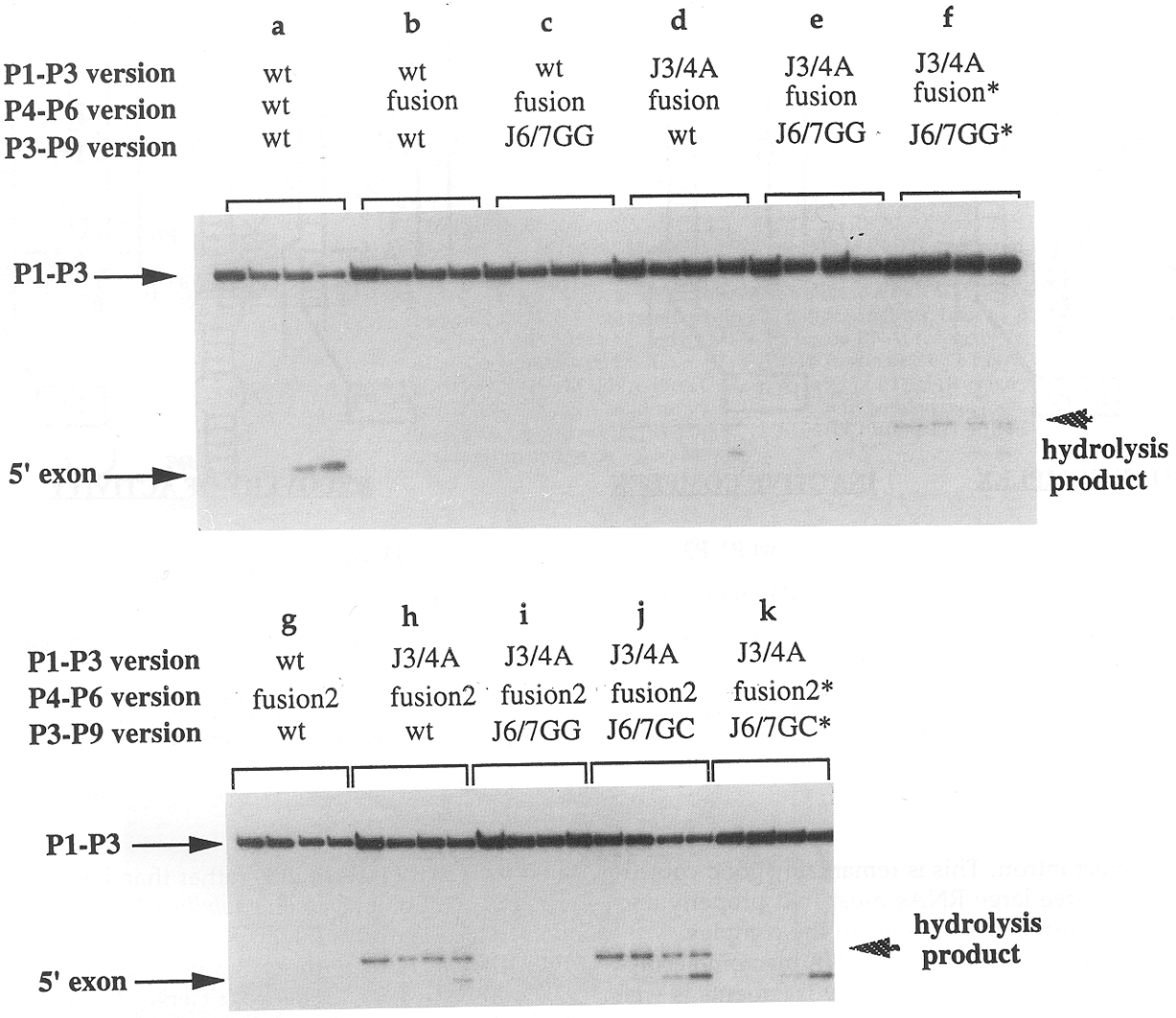

FIGURE 6. Recovery of catalytic activity in RNA complexes containing the P4–P6 fusion RNA and nucleotides from joining regions J3/4 and J6/7. Autoradiograms of 10% gels are shown; upper and lower arrows at left indicate the positions of full-length P1–P3 RNA substrate and the 20-nucleotide cleaved 5′ exon sequence, respectively. Hatched arrow at right indicates mobility of a hydrolysis product that arises in some cases during preincubation of the RNAs prior to reaction. Sets of four timepoints taken after 0, 5, 10, and 30 min of reaction at 40 °C are shown; 1 nM 5′-^{32}P-labeled P1–P3 RNA and 100 nM P4–P6 (or variant) and P3–P9(*Sca* I) (or variant) RNAs were used unless otherwise stated. Wt, original RNA constructs shown in Figure 1; fusion, circularly permuted P4–P6 with 5′ and 3′ ends in L6 (see Fig. 4A); J3/4A, P1–P3 sequence plus nucleotides AAU added at 3′ end; J6/7GG, P3–P9 sequence plus GGUCA added at 5′ end; fusion2, circularly permuted P4–P6 with base pair 2 in P4 changed from C-G to G-C; J6/7GC, P3–P9 sequence plus GCA added at 5′ end; asterisks, reactions in which 1 μM rather than 0.1 μM of the indicated RNA was used.

1991; Purohit & Stern, 1994). The 160-nucleotide P4–P6 region of the *Tetrahymena* Group I intron is known to form an independent tertiary structure both within the intron and as a separate molecule. The data presented here do not directly address the question of whether the other proposed domain of the core, P3–P9, is also an independently folded domain. This RNA may require interaction with P4–P6 to form its active structure, as has been suggested in studies of the folding of the intact intron (Celander & Cech, 1991; Laggerbauer et al., 1994; Zarrinkar & Williamson, 1994).

The P3–P9 RNA probably requires interaction with the P1–P3 RNA to fold because the P3 helix is formed by base-pairing between these molecules. Interestingly, the 3′ helices P9.1 and P9.2 are required for catalytic activity of the domain complex. These stems are not highly conserved phylogenetically and can be deleted from the intron with only small effects on activity if the reaction conditions are sufficiently stabilizing (Szostak, 1986; Barfod & Cech, 1988). This observation is consistent with data from chemical protection studies of a truncated intron that showed that deletion of P9.1 and P9.2 destabilizes the P3–P7 region of the catalytic core (Laggerbauer et al., 1994). In the separated domains, however, P9.1 and P9.2 appear to greatly stabilize the interaction between the P1–P3 and P3–P9

RNAs, consistent with the proposed base-pairing of the hairpin loops of P9.1 and P2.1 (Been et al., 1987; Banerjee et al., 1993).

We tested the activity of a particularly interesting P4–P6 mutant in which the 5′ and 3′ ends were circularly permuted to the loop L6. This "P4–P6 fusion" molecule was originally designed to test the idea that the P4 and P6 helices are coaxially stacked in the native P4–P6 RNA; it was found to fold like the native P4–P6 domain (Murphy et al., 1994). The P4–P6 fusion RNA was active in our reconstitution assay, although not with the original P1–P3 and P3–P9 constructs. Nucleotides in the joining regions J3/4 and J6/7, missing from the P4–P6 fusion molecule, had to be included on the P1–P3 and P3–P9 RNAs to restore activity. One explanation for this result is that these nucleotides, which are proposed to engage in triple-strand interactions with stems P4 and P6, are additionally involved in tertiary interactions between the domains of the intron. These interactions might be necessary to achieve the proper orientation of the two domains of the core, or they might have an even more direct role in catalysis.

The separation of the catalytic core of the *Tetrahymena* intron into tertiary domains provides a useful approach for determining structural versus catalytic requirements for intron function. Domain RNAs containing mutations in regions directly involved in catalysis would be expected to form stable, but inactive, complexes. Domain RNAs containing structural defects would be expected to interact much more weakly in a complex.

The organization of RNA into domains of tertiary structure is emerging as a common theme in large structured molecules such as self-splicing introns (Groups I and II), ribonuclease P, and ribosomal RNAs. This organization may be reflected in the features of some ribonucleoproteins as well, such as the individual snRNP particles that interact within the spliceosome during messsenger RNA splicing. Both the spliceosome and the ribosome are assembled from component ribonucleoprotein particles that interact transiently to perform a reaction. The finding that a Group I intron active site can be assembled from smaller structured units of RNA adds credence to the possibility that there may have been a primitive spliceosome and a primitive ribosome without any proteins.

MATERIALS AND METHODS

Materials

Taq polymerase was purchased from Boehringer Mannheim. T7 RNA polymerase was prepared by J.A.D. according to a procedure developed by Dr. Steve Schultz (pers. comm.).

Plasmid template construction

Plasmid pP3P9, which encodes the P3–P9 RNA, was constructed from pTZL-21 (Grosshans & Cech, 1991) using the phagemid mutagenesis technique of Kunkel et al. (1987). Nucleotides 1–261 of the *Tetrahymena* L-21 *Sca* I ribozyme sequence were deleted. The first base pair in P7 was changed from C-G to G-C so that the transcript would begin with a G, as required by T7 RNA polymerase. This base pair change does not adversely affect ribozyme activity (Couture et al., 1990). Plasmids pP4P6 and pP4P6fusion were provided by Felicia Murphy (Murphy & Cech, 1993; Murphy et al., 1994). Sequences were confirmed by dideoxy sequencing.

PCR template construction

Templates for substrate RNAs P1–P3 and J3/4A were prepared by PCR amplification of the specified region of plasmid pTZΔ12IVS (Woodson & Cech, 1991). Each contained the T7 RNA polymerase promoter followed by 20 nucleotides of the natural 5′ exon sequence. A *Bsa* I restriction site was positioned at the 3′ end of the template such that digestion of the PCR fragment produced templates ending at nucleotide 103 for P1–P3 and nucleotide 106 for J3/4A. The template for P4–P6 fusion2 RNA was produced by PCR amplification of pP4P6 to produce an identical molecule with base pair 2 in P4 changed from G-C to C-G. Templates for J6/7GG and J6/7GC RNAs were produced by PCR amplification of pP3P9 to produce identical molecules with 5′-GGUCA added (J6/7GG) or 5′-GCA added (J6/7GC).

RNA preparation

Plasmids were digested with *Sca* I or *Nhe* I (pP3P9) or *Ear* I (pP4P6 and pP4P6fusion). PCR templates were digested with *Bsa* I. Transcription and gel purification were performed essentially as described (Latham et al., 1990). Radioactive labeling of RNAs at their 5′ ends with ^{32}P was performed as described (Latham et al., 1990).

Cleavage reactions

RNAs were preincubated in a buffer containing 30 mM Tris-HCl, pH 7.5, 5 mM $MgCl_2$, and 5 mM spermidine for 10 min at 50 °C. Typical concentrations for each RNA were 1 nM P1–P3, 100 nM P4–P6, and 100 nM P3–P9. Following this incubation, samples were transferred to 40 °C for 5 min, and then the concentrations of $MgCl_2$ and guanosine were adjusted with prewarmed solutions to 80 mM and 5 mM, respectively, to initiate the reaction. Aliquots were removed at each time point and quenched on ice with the addition of an equal volume of a buffer containing 10 mM Tris-HCl, pH 7.5, 1 mM EDTA, 10 mM boric acid, 90% formamide, and 0.4% each of xylene cyanole and bromophenol blue. Reaction products were separated on 10% polyacrylamide gels containing 7 M urea. Gels were dried and quantitated using a PhosphorImager (Molecular Dynamics Corp.). Kinetic data were plotted using SigmaPlot (Jandel Scientific).

ACKNOWLEDGMENTS

We thank François Michel for helpful advice on reconstruction of the P4-J6/7 triple helix, and Thomas Griffin and Jamie Cate for critical reading of the manuscript. J.A.D. is a Lucille P. Markey Scholar in Biomedical Science and this work was sup-

ported in part by a grant from the Lucille P. Markey Charitable Trust. T.R.C. is an Investigator of the Howard Hughes Medical Institute and an American Cancer Society Professor. We thank the W.M. Keck Foundation for their generous support of RNA research at the University of Colorado at Boulder.

Received December 27, 1994; returned for revision January 9, 1995; revised manuscript received January 14, 1995

REFERENCES

Bachl J, Schmelzer C. 1990. Effect of deletions at structural domains of group II intron bI1 on self-splicing in vitro. *J Mol Biol 212*: 113–125.

Banerjee AR, Jaeger JA, Turner DH. 1993. Thermal unfolding of a group I ribozyme: The low-temperature transition is primarily disruption of tertiary structure. *Biochemistry 32*:153–163.

Barfod ET, Cech TR. 1988. Deletion of nonconserved helices near the 3′ end of the rRNA intron of *Tetrahymena thermophila* alters self-splicing but not core catalytic activity. *Genes & Dev 2*:652–663.

Beebe JA, Fierke CA. 1994. A kinetic mechanism for cleavage of precursor $tRNA^{Asp}$ catalyzed by the RNA component of *Bacillus subtilis* ribonuclease P. *Biochemistry 33*:10294–10304.

Been MD, Barfod ET, Burke JM, Price JV, Tanner NK, Zaug AJ, Cech TR. 1987. Structures involved in *Tetrahymena* rRNA self-splicing and RNA enzyme activity. *Cold Spring Harbor Symp Quant Biol 52*:147–157.

Cech TR. 1990. Self-splicing of group I introns. *Annu Rev Biochem 59*:543–568.

Cech TR, Damberger SH, Gutell RR. 1994. Representation of the secondary and tertiary structure of group I introns. *Nature Struct Biol 1*:273–280.

Celander DW, Cech TR. 1991. Visualizing the higher order folding of a catalytic RNA molecule. *Science 251*:401–407.

Chambers RW. 1971. On the recognition of tRNA by its aminoacyl-tRNA ligase. *Prog Nucleic Acid Res Mol Biol 11*:489–525.

Chastain M, Tinoco I Jr. 1992. A base-triple structural domain in RNA. *Biochemistry 31*:12733–12741.

Chastain M, Tinoco I Jr. 1993. Nucleoside triples from the group I intron. *Biochemistry 32*:14220–14228.

Couture S, Ellington AD, Gerber AS, Cherry JM, Doudna JA, Green R, Hanna M, Pace U, Rajagopal J, Szostak JW. 1990. Mutational analysis of conserved nucleotides in a self-splicing group I intron. *J Mol Biol 215*:345–358.

Dib-Hajj SD, Boulanger SC, Hebbar SK, Peebles CL, Franzen JS, Perlman PS. 1993. Domain 5 interacts with domain 6 and influences the second transesterification reaction of Group II intron self-splicing. *Nucleic Acids Res 21*:1797–1804.

Doudna JA, Couture S, Szostak JW. 1991. A multisubunit ribozyme that is a catalyst of and a template for complementary strand RNA synthesis. *Science 251*:1605–1608.

Doudna JA, Grosshans C, Gooding A, Kundrot CE. 1993. Crystallization of ribozymes and small RNA motifs by a novel sparse matrix approach. *Proc Natl Acad Sci USA 90*:7829–7833.

Doudna JA, Szostak JW. 1989. RNA-catalyzed synthesis of complementary strand RNA. *Nature 339*:519–522.

Downs WD, Cech TR. 1990. An ultraviolet-inducible adenosine-adenosine crosslink reflects the catalytically-active structure of the *Tetrahymena* ribozyme. *Biochemistry 29*:5605–5613.

Downs WD, Cech TR. 1994. A tertiary interaction in the *Tetrahymena* intron contributes to selection of the 5′ splice site. *Genes & Dev 8*:1198–1211.

Goldschmidt-Clermont M, Choquet Y, Girard-Bascou J, Michel F, Schirmer-Rahire M, Rochaix JD. 1991. A small chloroplast RNA may be required for *trans*-splicing in *Chlamydomonas reinhardtii*. *Cell 65*:135–143.

Green R, Szostak JW. 1994. In vitro genetic analysis of the hinge region between helical elements P5–P4–P6 and P7–P3–P8 in the *sunY* group I self-splicing intron. *J Mol Biol 235*:140–155.

Grosshans CA, Cech TR. 1991. A hammerhead ribozyme allows synthesis of a new form of the *Tetrahymena* ribozyme homogeneous in length with a 3′ end blocked for transesterification. *Nucleic Acids Res 19*:3875–3880.

Harris ME, Nolan JM, Malhotra A, Brown JW, Harvey SC, Pace NR. 1994. Use of photoaffinity crosslinking and molecular modeling to analyze the global architecture of ribonuclease P RNA. *EMBO J 13*:3953–3963.

Heuer TS, Chandry PS, Belfort M, Celander DW, Cech TR. 1991. Folding of group I introns from bacteriophage T4 involves internalization of the catalytic core. *Proc Natl Acad Sci USA 88*:11105–11109.

Jacobson RH, Zhang XJ, DuBose RF, Matthews BW. 1994. Three-dimensional structure of beta-galactosidase from *E. coli*. *Nature 369*:761–766.

Jaeger L, Westhof E, Michel F. 1993. Monitoring of the cooperative unfolding of the *sunY* group I intron of bacteriophage T4. *J Mol Biol 234*:331–346.

Jarrell KA, Dietrich RC, Perlman PS. 1988. Group II intron domain 5 facilitates a *trans*-splicing reaction. *Mol Cell Biol 8*:2361–2366.

Kean JM, Draper DE. 1985. Secondary structure of a 345-base RNA fragment covering the S8/S15 protein binding domain of *Escherichia coli* 16S ribosomal RNA. *Biochemistry 24*:5052–5061.

Kunkel TA, Roberts JD, Zakour RA. 1987. Rapid and efficient site-specific mutagenesis without phenotypic selection. *Methods Enzymol 154*:367–382.

Laggerbauer B, Murphy FL, Cech TR. 1994. Two major tertiary folding transitions of the *Tetrahymena* catalytic RNA. *EMBO J 13*: 2669–2676.

Latham JA, Cech TR. 1989. Defining the inside and outside of a catalytic RNA molecule. *Science 245*:276–282.

Latham JA, Zaug AJ, Cech TR. 1990. Self-splicing and enzymatic cleavage of RNA by a group I intervening sequence. *Methods Enzymol 181*:558–569.

Michel F, Ellington AD, Couture S, Szostak JW. 1990. Phylogenetic and genetic evidence for base triples in the catalytic domain of group I introns. *Nature 347*:578–580.

Michel F, Hanna M, Green R, Bartel DP, Szostak JW. 1989a. The guanosine binding site of the *Tetrahymena* ribozyme. *Nature 342*:391–395.

Michel F, Jaeger L, Westhof E, Kuras R, Tihy F, Xu MQ, Shub DA. 1992. Activation of the catalytic core of a group I intron by a remote 3′ splice junction. *Genes & Dev 6*:1373–1385.

Michel F, Umesono K, Ozeki H. 1989b. Comparative and functional anatomy of Group II catalytic introns—A review. *Gene 82*:5–30.

Michel F, Westhof E. 1990. Modelling of the three-dimensional architecture of group I catalytic introns based on comparative sequence analysis. *J Mol Biol 216*:585–610.

Murphy FL, Cech TR. 1993. An independently folding domain of tertiary structure within the *Tetrahymena* ribozyme. *Biochemistry 32*:5291–5300.

Murphy FL, Cech TR. 1994. GAAA tetraloop and conserved bulge stabilize tertiary structure of a Group I intron domain. *J Mol Biol 236*:49–63.

Murphy FL, Wang YH, Griffith JD, Cech TR. 1994. Coaxially stacked RNA helices in the catalytic center of the *Tetrahymena* ribozyme. *Science 265*:1709–1712.

Noller HF. 1991. Ribosomal RNA and translation. *Annu Rev Biochem 60*:191–227.

Pan T. 1994. Higher order structure and domain analysis of the ribozyme from *Bacillus subtilis* ribonuclease P. *Biochemistry*. Forthcoming.

Purohit P, Stern S. 1994. Interactions of a small RNA with antibiotic and RNA ligands of the 30S subunit. *Nature 370*:659–662.

Pyle AM, Green J. 1994. Building a kinetic framework for group II intron ribozyme activity: Quantitation of interdomain binding and reaction rate. *Biochemistry 33*:2716–2725.

Pyle AM, Murphy FL, Cech TR. 1992. RNA substrate binding site in the catalytic core of the *Tetrahymena* ribozyme. *Nature 358*: 123–128.

Strobel SA, Cech TR. 1993. Tertiary interactions with the internal guide sequence mediate docking of the P1 helix into the catalytic core of the *Tetrahymena* ribozyme. *Biochemistry 32*:13593–13604.

Szostak JW. 1986. Enzymatic activity of the conserved core of a group I self-splicing intron. *Nature 322*:83–86.

Uhlenbeck OC. 1987. A small catalytic oligoribonucleotide. *Nature 328*:596–600.

Van der Horst G, Christian A, Inoue T. 1991. Reconstitution of a group I intron self-splicing reaction with an activator RNA. *Proc Natl Acad Sci USA 88*:184–188.

Wang JF, Cech TR. 1992. Tertiary structure around the guanosine-binding site of the *Tetrahymena* ribozyme. *Science 256*:526–529.

Wang JF, Downs WD, Cech TR. 1993. Movement of the guide sequence during RNA catalysis by a group I ribozyme. *Science 260*: 504–508.

Wang YH, Murphy FL, Cech TR, Griffith JD. 1994. Visualization of a tertiary structural domain of the *Tetrahymena* Group I intron by electron microscopy. *J Mol Biol 236*:64–71.

Weitzmann CJ, Cunningham PR, Nurse K, Ofengand J. 1993. Chemical evidence for domain assembly of the *Escherichia coli* 30S ribosome. *FASEB J 7*:177–180.

Woodson SA, Cech TR. 1991. Alternative secondary structures in the 5′ exon affect both forward and reverse self-splicing of the *Tetrahymena* intervening sequence RNA. *Biochemistry 30*:2042–2050.

Yarus M, Illangesekare M, Christian E. 1991. An axial binding site in the *Tetrahymena* precursor RNA. *J Mol Biol 222*:995–1012.

Zarrinkar PP, Williamson JR. 1994. Kinetic intermediates in RNA folding. *Science 265*:918–924.